Eur. Phys. J. A **10**, 41–47 (2001)

THE EUROPEAN PHYSICAL JOURNAL A

High-spin states in neutron-rich Dy isotopes populated in deep-inelastic reactions

X. Liang[1,a], R. Chapman[1], K.-M. Spohr[1], M.B. Smith[1,b], P. Bednarczyk[2,5], S. Naguleswaran[5], F. Haas[5], G. de Angelis[4], S.M. Campbell[1], P.J. Dagnall[3], M. Davison[1], G. Duchêne[5], Th. Kröll[6], S. Lunardi[6], and D.J. Middleton[1]

[1] Division of Electronic Engineering and Physics, University of Paisley, Paisley PA1 2BE, UK
[2] H. Niewodniczański Institute of Nuclear Physics, PL–31–342 Kraków, Poland
[3] Department of Physics and Astronomy, University of Manchester, Manchester M13 9PL, UK
[4] INFN, LNL, I–35020 Legnaro, Italy
[5] IReS, F–67037 Strasbourg Cedex 2, France
[6] Dipartimento di Fisica and INFN, Sezione di Padova, 1-35131 Padova, Italy

Received: 20 October 2000 / Revised version: 7 December 2000
Communicated by D. Schwalm

Abstract. High-spin states in neutron-rich Dy isotopes, populated in deep-inelastic processes produced by the interaction of 234 MeV ^{37}Cl ions with a ^{160}Gd target, have been studied using the highly sensitive EUROBALL IV gamma-ray detector array. The previously known level schemes for ^{159,160,161,162}Dy have been extended to significantly higher spin ($\leq 30\hbar$) and the $i_{13/2}$ band crossing in ^{159}Dy has been observed for the first time. The experimental results are discussed within the framework of cranked shell model and projected shell model calculations with particular reference to the observed delayed band crossing in ^{162}Dy.

PACS. 23.20.Lv Gamma transitions and level energies – 27.70.+q $150 \leq A \leq 189$

1 Introduction

Neutron-rich nuclei are of particular current interest since they are predicted to reveal new aspects of nuclear structure associated with an excess of neutrons, such as a modified residual interaction, a neutron skin, and exotic modes of excitation. A challenge lies, however, in their production, since the majority of reaction mechanisms do not produce neutron-rich isotopes. By contrast, deep-inelastic reactions can access nuclei with appreciably higher N/Z ratios [1], and this has resulted in an increasing interest in the use of such reactions to populate neutron-rich nuclei [2–6]. Takai *et al.* [7] were among the first to utilize discrete γ-ray spectroscopy in the study of deep-inelastic reactions. In their experiment, high-spin states in ^{170}Yb were identified up to a spin of $20\hbar$. In relation to the present region of interest, Asztalos *et al.* [8] recently undertook a series of experiments using deep-inelastic reactions to populate yrast states in neutron-rich Yb(A = 172–178) and Sm(A = 152–156) isotopes with spin up to $22\hbar$. In the deep-inelastic experiment discussed here, new γ transitions were identified in several neutron-rich Dy isotopes. In total, seven Dy isotopes have been populated, namely those with $A = 156$ to 162. In this paper we focus attention on the yrast and near-yrast decay sequences of the neutron-rich isotopes, ^{159,160,161,162}Dy. The properties of the observed decay sequences are interpreted in terms of the results of cranked shell model and recent projected shell model calculations.

2 Experimental details and results

High-spin states in Dy isotopes were populated in the interaction of a 234 MeV beam of ^{37}Cl ions delivered by the VIVITRON at IReS, Strasbourg, with a ^{160}Gd target. The target, isotopically enriched to 98.2% in ^{160}Gd, was of thickness $12\,\mathrm{mg}\cdot\mathrm{cm}^{-2}$ and was backed with $40\,\mathrm{mg}\cdot\mathrm{cm}^{-2}$ of isotopically enriched ^{208}Pb(99.47%). The target was sufficiently thick to stop all recoiling reaction fragments; the experimental objective was to detect gamma rays from stopped fragments, thus avoiding Doppler-broadening effects in the measured energy spectrum of γ-rays. Study of the γ-de-excitation of the products of deep-inelastic reactions is difficult because yields are generally very low. Gamma-rays were detected using the highly sensitive EUROBALL IV array [9]. Experimental data were taken during a three day run. The electronic trigger condition was

[a] e-mail: lian-ph0@wpmail.paisley.ac.uk
[b] *Present address*: Department of Physics and Astronomy, Rutgers University, New Brunswick, New Jersey 08903, USA

such that when seven Ge signals before Compton suppression or five Ge signals before Compton suppression and nine BGO inner ball element signals were in time coincidence, the "event" was accepted and subsequently written to tape. The data were sorted off-line into a γ-γ-γ cube and analysed using the RADWARE code [10]. In the analysis of the EUROBALL data a γ-γ-γ cube was constructed without conditions being imposed relating to timing or to the inner BGO ball fold or sum energy.

One of the goals of our studies in the rare-earth region is to populate yrast and near-yrast decay sequences of neutron-rich nuclei to moderately high spin ($\sim 30\hbar$). In this work, analysis of the data initially involved setting gates on known γ-ray transitions. One new tentative transition (713 keV(17) $\rightarrow 16^+$) has been identified in ^{158}Dy, the other 21 new transitions are associated with the yrast and near-yrast decay sequences of ^{159}Dy, ^{160}Dy, ^{161}Dy and ^{162}Dy.

The yrast sequence of ^{159}Dy was known previously [11–13] up to spin $45/2^+$. In the present work, the band has been extended to a spin of $61/2^+$ and the first band crossing observed for the first time. In earlier published work [14–16], the yrast sequence in ^{160}Dy was established up to spin 18^+. However, in the more recent work reported in ref. [17], the yrast sequence was observed to spin 28^+, although no level scheme was presented. In the present work, the band has been established to spin 28^+. One additional decay sequence has also been observed up to spin (18^+). In ^{161}Dy, we have extended the $5/2[642], \alpha = +\frac{1}{2}$ band from the previously known [18–20] spin $33/2^+$ to $53/2^+$, and also added a new transition to the $5/2[642], \alpha = -\frac{1}{2}$ decay sequence. In ^{161}Dy the unfavoured component of the rotational sequence based on the 5/2[642] configuration is, in the present work, populated only to spin $35/2^+$, while the favoured component is seen to spin $53/2^+$. The relatively weak population of high-spin states of the unfavoured sequence is probably mainly a consequence of the increasing signature splitting of the two decay sequences which occurs with increasing spin. The very weak population of the unfavoured sequence of the 5/2[642] band in ^{159}Dy may be explained in the same way. However, we cannot entirely exclude the possibility that, in the deep-inelastic process, the feeding mechanism is to some extent different from that of heavy-ion induced fusion evaporation reactions. In ^{162}Dy one additional transition (741 keV) has been added; we tentatively assign this as the $20^+ \rightarrow 18^+$ transition in the yrast sequence.

The placement of the new transitions in the decay sequences was based on coincidence and intensity relationships. Examples of gated coincidence spectra which show some of the new cascades are presented in fig. 1. The intensity relationships were also used to confirm that the observed γ-ray peaks should be assigned to the Dy isotopes and not to the complementary fragments. The assignment of γ-ray transitions to the isotopes of Dy is based on an examination of many gated spectra. In figs. 1 (a), (b), (d) and (e) there is a common peak of energy 429 keV marked by "*"; it has been assigned to the corresponding projectile-like nucleus ^{34}P. Observation of a

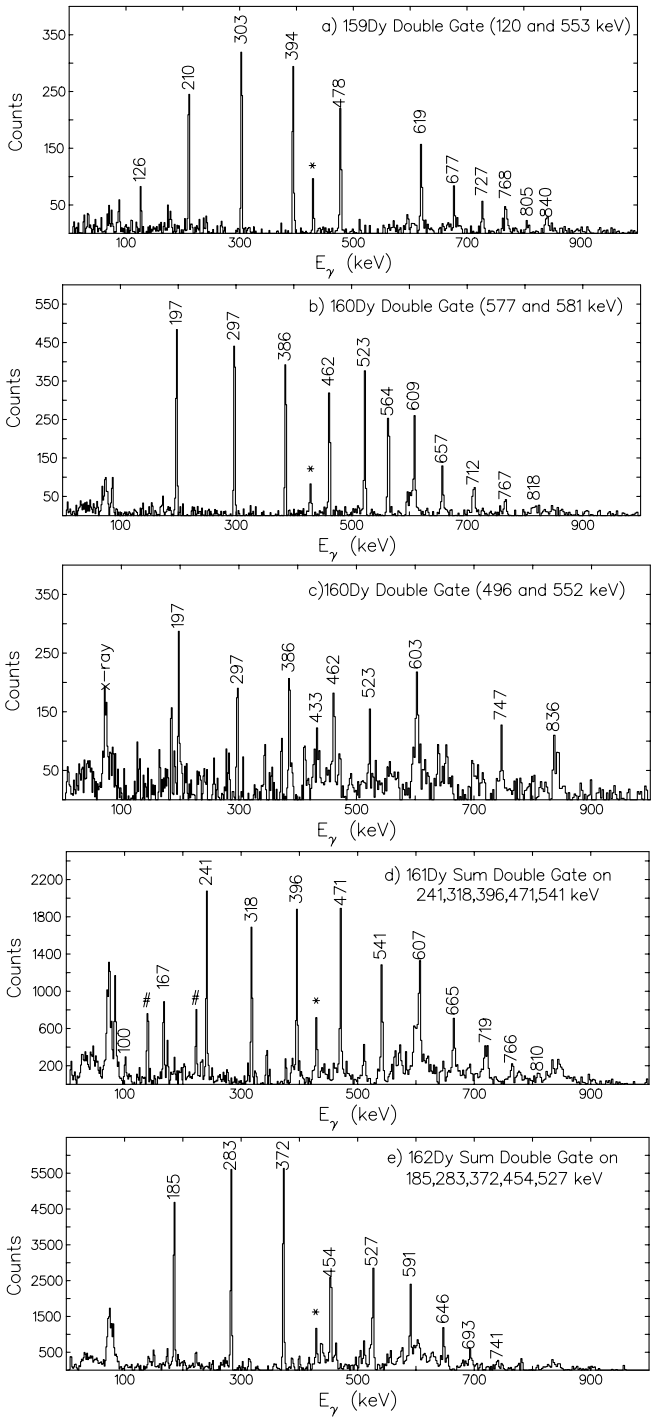

Fig. 1. Examples of gated spectra for ^{159}Dy, ^{160}Dy, ^{161}Dy and ^{162}Dy.

^{34}P γ-ray transition in coincidence with rotational sequences in ^{159}Dy, ^{160}Dy, ^{161}Dy and ^{162}Dy, demonstrates that 4n, 3n, 2n and 1n evaporation has occurred. In each spectrum, there is a broad peak around 75 keV which we assign as the Pb X-rays in random coincidence with Dy γ-rays. For de-excitation of high-spin states of the Dy isotopes studied here, the lifetimes of the states be-

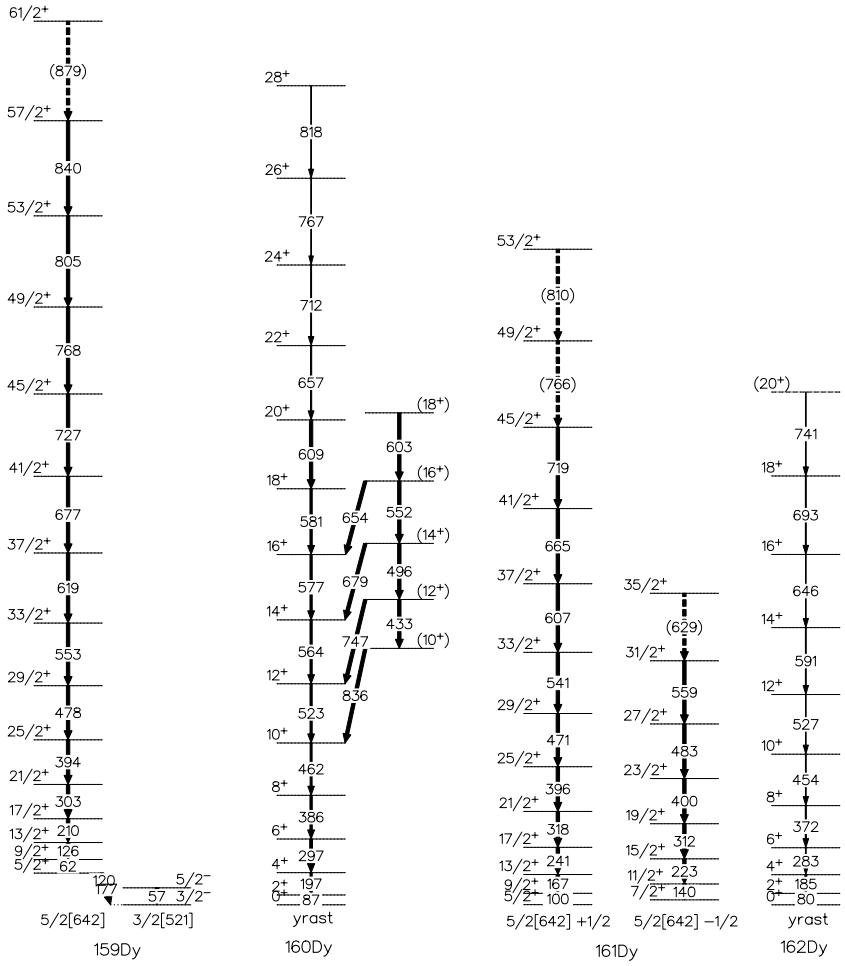

Fig. 2. Partial level schemes of Dy isotopes.

come comparable with the slowing-down times of the Dy ions (estimated $\frac{v}{c} \sim 1.5\%$) in the target material for lifetimes less than about 1 ps. There is some experimental evidence of Doppler lineshapes for gamma-ray photopeaks corresponding to the depopulation of states of spin greater than about $20\hbar$ (for example the 677 keV line in the spectrum of fig. 1(a) and the 657 keV line in the spectrum of fig. 1(b)). Of course, setting gates on the stopped components of γ-ray lineshapes, as has been the practice here, has a distorting effect on the measured lineshapes of coincident γ-rays, thus reducing Doppler-related effects. The spectrum of fig. 1(a) corresponds to double gating on the 120 keV and 553 keV transitions within the yrast sequence of ^{159}Dy; several new γ-ray transitions at 768 keV, 805 keV, 840 keV and (tentatively) 879 keV are clearly observed and have been assigned to ^{159}Dy. The spectrum of fig. 1(b) corresponds to gating on the 577 keV and 581 keV transitions within the yrast sequence of ^{160}Dy; new γ-ray transitions at 609, 657, 712, 767 and 818 keV are clearly seen. The spectrum of fig. 1(c) corresponds to gating on the 496 keV and 552 keV γ-ray photopeaks from the side band of ^{160}Dy; the quality of the gated spectrum is poor compared to the others displayed in fig. 1. In the spectrum of fig. 1(c), the yrast decay sequence transitions at 197, 297, 386, 462 and 523 keV and the connecting transitions between the two bands at 747 keV and 836 keV are clearly seen. The two connecting transitions at 679 keV and 654 keV are blocked by the gating transitions. In addition, two transitions at 433 keV and 603 keV in the side band are clearly seen. In the paper by Riezebos *et al.* [16], a doublet line 836 keV$((11^-) \rightarrow 10^+)$/837 keV$((10^+) \rightarrow 10^+)$ was observed. In the present work, by double gating on previously known transitions 462 keV$(10^+ \rightarrow 8^+)$ and 433 keV$((12^+) \rightarrow (10^+))$, a transition of energy 836 keV is clearly seen, thus removing any ambiguity in relation to its placing in the level sequence. The spectrum for ^{161}Dy constructed by summing all double-gated spectra involving all combinations of the transitions at 241 keV, 318 keV, 396 keV, 471 keV and 541 keV is shown in fig. 1(d). These transitions were earlier [18–20] identified as belonging to the favoured signature of the 5/2[642] band. From the spectrum of fig. 1(d), we can add several new transitions to the band; they are at 607, 665, 719, 766 and 810 keV. A new possible transition at 629 keV has also been tentatively added to the unfavoured signa-

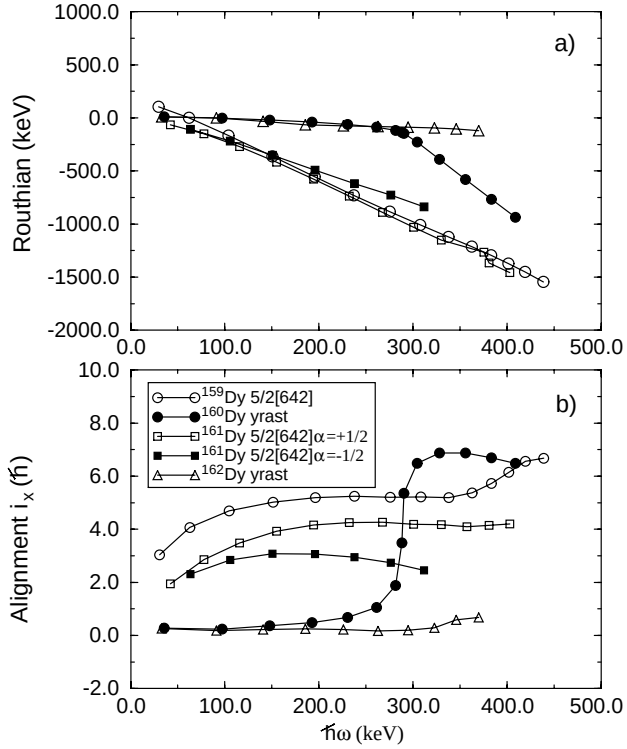

Fig. 3. (a) Experimental Routhians and (b) quasiparticle alignment i_x for ^{159}Dy, ^{160}Dy, ^{161}Dy and ^{162}Dy, plotted as a function of rotational frequency $\hbar\omega$.

ture of the 5/2[642] band in ^{161}Dy (see fig. 2). There are two peaks marked by "#" in fig. 1(d); they are impurity transitions which have been brought in by the gating condition. The spectrum of fig. 1(e) corresponds to summing all double-gated spectra involving the transitions at 185, 283, 372, 454 and 527 keV in the yrast sequence of ^{162}Dy. A new transition at 741 keV has been tentatively added to the top of the sequence.

The level schemes of $^{159-162}$Dy resulting from the present work are presented in fig. 2.

3 Discussion

Figure 3 (a) shows the experimental Routhians and (b) the quasiparticle aligned angular momenta for ^{159}Dy, ^{160}Dy, ^{161}Dy and ^{162}Dy, plotted as a function of rotational frequency $\hbar\omega$. For ^{159}Dy, a reference has been subtracted with Harris parameters $\mathcal{J}^{(0)} = 30$ MeV$^{-1}\hbar^2$ and $\mathcal{J}^{(1)} = 120$ MeV$^{-3}\hbar^4$. For ^{160}Dy, the reference parameters were $\mathcal{J}^{(0)} = 32$ MeV$^{-1}\hbar^2$ and $\mathcal{J}^{(1)} = 116$ MeV$^{-3}\hbar^4$. For ^{161}Dy and ^{162}Dy, a common reference has been subtracted with Harris parameters $\mathcal{J}^{(0)} = 35$ MeV$^{-1}\hbar^2$ and $\mathcal{J}^{(1)} = 116$ MeV$^{-3}\hbar^4$. The reference configurations were based on Harris-parameter fits to the energies of the yrast sequences below the first band crossing in the even-A Dy isotopes.

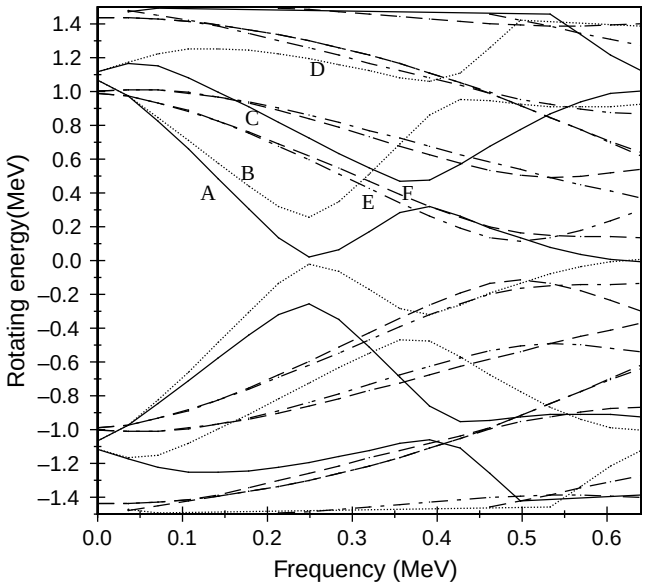

Fig. 4. CSM calculations for neutron orbitals in ^{160}Dy.

The rotational sequences have been interpreted within the framework of the Cranked Shell Model [21]. For ^{160}Dy, fig. 4 shows the Routhians for quasineutrons, calculated with the cranked shell model (CSM) using deformation parameters $\varepsilon_2 = 0.248$, $\varepsilon_4 = -0.020$ and $\gamma = 0°$ taken from ref. [22]. The pairing gap parameter, Δ, was calculated from known masses, using the formula of Bohr and Mottelson [23]. Cranked shell model calculations were also performed for ^{159,161,162}Dy, but not presented here. In fig. 4 the various curves are labelled according to parity and signature (π, α) as follows: $(+,+\frac{1}{2})$ solid lines (A, C), $(+,-\frac{1}{2})$ dotted lines (B, D), $(-,+\frac{1}{2})$ dot-dashed line (E) and $(-,-\frac{1}{2})$ dashed line (F). The results of the cranked shell model calculations for ^{160}Dy show that at a rotational frequency of 0.26 MeV the fully paired yrast configuration (the quasiparticle vacuum) is crossed by the more energetically favourable two-quasineutron configuration, based on the $i_{13/2}$ neutron orbitals 5/2[642] (the AB neutron crossing). For rotational frequencies in excess of 0.26 MeV the yrast sequence is now based on a two-quasineutron $\nu(i_{13/2})^2$ configuration. At a rotational frequency of about 0.38 MeV a second pair of $i_{13/2}$ neutrons aligns (the BC neutron crossing) and this can be observed, for example, as a band crossing in negative-parity AE decay sequences in which the A orbital is occupied. The Coriolis and centrifugal forces are responsible for the alignment of these high-$j(i_{13/2})$ orbitals. The lowest negative-parity orbitals (labelled E and F), based on the Nilsson configuration 3/2[521], are less affected by the nuclear rotation and here quasiparticle alignment does not occur until a rotational frequency of about 0.50 MeV is reached, beyond the limits of observation of the present experiment.

For ^{159}Dy, a band crossing at a frequency ($\hbar\omega_c$) of 0.35 MeV is observed for the first time in the present work. Comparison of the experimental crossing frequency

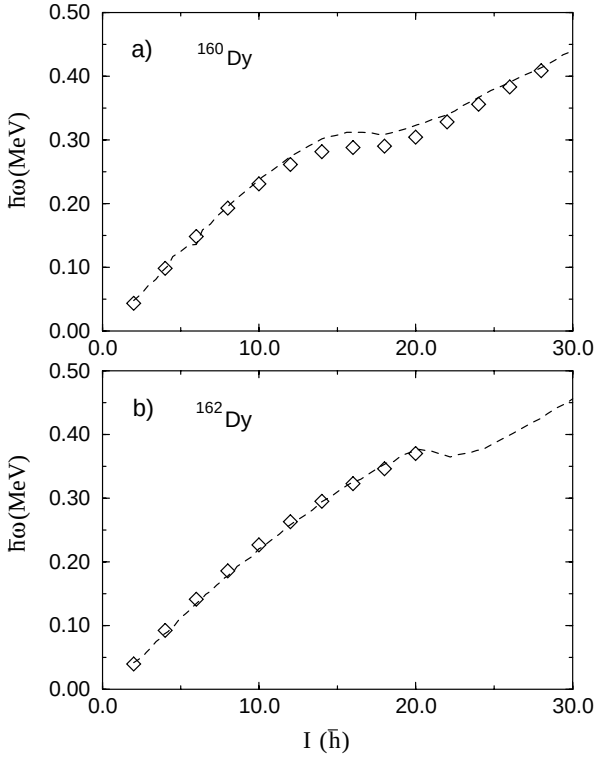

Fig. 5. Angular frequency $\hbar\omega$ *versus* angular momentum I for (a) ^{160}Dy and (b) ^{162}Dy. The PSM results using enlarged deformations are presented as dashed lines. Experimental data are represented by diamonds.

Table 1. A comparison of experimental and CSM calculations of ^{159}Dy, ^{160}Dy, ^{161}Dy and ^{162}Dy.

		Experiment	CSM
^{159}Dy			
$i_{\rm A}(\hbar)$		5.2 ± 0.1	5.33
$\hbar\omega_{\rm c}$ for BC crossing			
(MeV)		0.35 ± 0.03	0.36
$\Delta i_{\rm BC}(\hbar)$		≥ 1.70	3.97
^{160}Dy			
$\hbar\omega_{\rm c}$ for AB crossing			
(MeV)		0.28 ± 0.01	0.26
$\Delta i_{\rm AB}(\hbar)$		6.9 ± 0.2	7.18
^{161}Dy			
$i_{\rm A}(\hbar)$		4.2 ± 0.2	4.71
$i_{\rm B}(\hbar)$		2.9 ± 0.2	3.64
$\hbar\omega_{\rm c}$ for BC crossing			
(MeV)		> 0.40	0.36
Signature Splitting	$\hbar\omega$ (MeV)		
(MeV)	0.100	0.020	0.030
	0.150	0.050	0.070
	0.200	0.100	0.130
	0.250	0.160	0.180
^{162}Dy			
$\hbar\omega_{\rm c}$ for AB crossing			
(MeV)		> 0.37	0.25

(fig. 3) with the results of CSM calculations suggests that the first crossing corresponds to the alignment of a BC neutron pair; the first predicted interaction, the AB crossing, is blocked in the rotational sequence of interest in ^{159}Dy since the A orbital is occupied below the first band crossing. The configuration of the band thus changes from a one-quasineutron configuration A(5/2[642]) to a three-quasineutron configuration ABC$(5/2[642] \otimes (\nu i_{13/2})^2)$ at a rotational frequency of 0.35 MeV.

For ^{160}Dy, an increase in alignment at a crossing frequency ($\hbar\omega_{\rm c}$) of 0.28 MeV, in agreement with earlier work [17], is clearly observed in fig. 3 and has been interpreted as an AB crossing.

In the case of ^{161}Dy, the favoured signature $\alpha = +\frac{1}{2}$ decay sequence has been observed in the present work for rotational frequencies up to 400 keV, while the $\alpha = -\frac{1}{2}$ unfavoured sequence has been established up to 315 keV. Experimentally, there is no strong evidence for a band crossing up to these frequencies. The two decay sequences exhibit signature splitting in the Routhians (fig. 3(a)).

For ^{162}Dy, the yrast sequence has been observed in the present work for rotational frequencies up to 370 keV. Although there is evidence for a slight increase in alignment around 350 keV, there is, from the present work, no strong evidence for a band crossing.

A more detailed comparison of the results of CSM calculations with the experimental data for ^{159}Dy, ^{160}Dy, ^{161}Dy and ^{162}Dy is presented in table 1. Experimental and theoretical crossing frequencies $\hbar\omega_{\rm c}$ are presented for each of the Dy isotopes. For the odd-A nuclei, the alignment values are presented before band crossing occurs. The alignment gains Δi, as a result of quasiparticle alignment, are also presented for ^{159}Dy and ^{160}Dy. Also shown are values of signature splitting for different rotational frequencies in ^{161}Dy. In general, the experimental and theoretical results agree well, except for the alignment gain $\Delta i_{\rm BC}$ in ^{159}Dy and the band crossing frequency $\hbar\omega_{\rm c}$ in ^{161}Dy and ^{162}Dy. For the alignment gain $\Delta i_{\rm BC}$ in ^{159}Dy, where the experimental value of $1.70\hbar$ (which is itself subject to some uncertainty as a consequence of the tentative nature of the $61/2^+ \rightarrow 59/2^+$ transition) falls short of the CSM value of $3.97\hbar$, it may be that we have not observed the full BC alignment gain in our experimental data, especially since this is a strong interaction crossing. For ^{161}Dy, the results of CSM calculations predict that a BC crossing should occur at rotational frequency of $\hbar\omega_{\rm c} = 0.36$ MeV. However, in the present work, there would appear to be no evidence for such a crossing for rotational frequencies up to 400 keV. A similar but more pronounced phenomenon is observed for ^{162}Dy. Here CSM calculations predict an AB crossing at $\hbar\omega_{\rm c} = 0.25$ MeV; however, there is no evidence of a crossing for rotational frequencies up to 370 keV. Clearly, the simple cranked shell model calculations are in this case inconsistent with experimental observation. It would, of course, be possible to increase the calculated band crossing frequencies

by increasing the quadrupole deformation parameter ε_2. For example, if ε_2 is increased by 20% from 0.261 to 0.313 for ^{162}Dy, the AB crossing frequency would increase from 0.25 MeV to 0.32 MeV.

The recent work by Velázquez *et al.* [24] has discussed backbending in Dy isotopes within the Projected Shell Model (PSM). The authors have shown that the use of an input deformation parameter, ϵ_2, 20% larger than the standard value, coupled with a slight reduction in effective charge, leads to an improved description of the yrast band energies. The authors have presented a comparison between the results of PSM calculations and experimental data for ^{160}Dy and ^{162}Dy up to spin $16\hbar$ and $18\hbar$, respectively. Figure 5 shows the comparison between the results of PSM calculations with enlarged deformation parameters and the present experimental data for ^{160,162}Dy. The inclusion of the experimental data presented here has extended the comparison for ^{160}Dy and ^{162}Dy up to spin $28\hbar$ and $20\hbar$, respectively . In fig. 5, the angular frequency $\hbar\omega$(defined as $\hbar\omega(I) = \frac{1}{2}[E(I) - E(I-2)]$), is plotted as a function of the spin I for the yrast sequences of ^{160}Dy and ^{162}Dy. For each plot, the dashed line corresponds to the results of PSM calculations with enlarged deformations, while the diamonds represent the present experimental data. From fig. 5, we are able to conclude that the results of PSM calculations using enlarged deformation parameters agree satisfactorily with the experimental data. In particular, the delayed AB band crossing in ^{162}Dy, which cannot satisfactorily be described within the context of the cranked shell model using "standard" parameters, is evident from the results of the PSM calculations. It would be interesting to extend the yrast sequence of ^{162}Dy to higher spin in order to extend the comparison with these calculations into the predicted band crossing region.

4 Conclusions

A total of 22 transitions have been added to the level schemes of five neutron-rich Dy isotopes. We have observed the BC crossing in ^{159}Dy for the first time and a comparison with the results of CSM calculations shows reasonable agreement for the crossing frequency for ^{159}Dy and ^{160}Dy, but not for ^{161}Dy and ^{162}Dy. For ^{159}Dy there is poor agreement between experiment and the results of CSM calculations for the quasiparticle alignment gain. The projected shell model results of Velázquez *et al.* [24] using enlarged deformations satisfactorily explain the delay in the AB band crossing for ^{162}Dy.

We would like to thank the technical staff of the VIVITRON accelerator laboratory for their support during the course of the experiment. This work was supported by the EPSRC (UK). We also would like to acknowledge support under the European Commission Programme "Training and Mobility of Researchers: Access to Large-Scale Facilities: Vivitron Accelerator and Associated Detectors" contract number ERBFMGECT980145. One of us (XL) acknowledges the receipt of a University of Paisley studentship and an ORS award during the course of this work. DJM acknowledges receipt of an EPSRC studentship.

References

1. H. Freiesleben, J.V. Kratz, Phys. Rep. **106**, 1 (1984).
2. B. Fornal, R.H. Mayer, I.G. Bearden, Ph. Benet, R. Broda, P.J. Daly, Z.W. Grabowski, I. Ahmad, M.P. Carpenter, P.B. Fernandez, R.V.F. Janssens, T.L. Khoo, T. Lauritsen, E.F. Moore, M. Drigert, Phys. Rev. C **49**, 2413 (1994).
3. P.H. Regan, T.M. Menezes, C.J. Pearson, W. Gelletly, C.S. Purry, P.M. Walker, S. Juutinen, R. Julin, K. Helariutta, A. Savelius, P. Jones, P. Jamsen, M. Muikku, P.A. Butler, G. Jones, P. Greenlees, Phys. Rev. C **55**, 2305 (1997).
4. K. Vetter, A.O. Macchiavelli, S.J. Asztalos, R.M. Clark, M.A. Deleplanque, R.M. Diamond, P. Fallon, R. Krucken, I.Y. Lee, R.W. MacLeod, G.J. Schmid, F.S. Stephens, Phys. Rev. C **56**, 2316 (1997).
5. I.Y. Lee, S. Asztalos, M.-A. Deleplanque, B. Cederwall, R.M. Diamond, P. Fallon, A.O. Macchiavelli, L. Phair, F.S. Stephens, G.J. Wozniak, S.G. Frauendorf, J.A. Becker, E.A. Henry, P.F. Hua, D.G. Sarantites, J.X. Saladin, C.H. Yu, Phys. Rev. C **56**, 753 (1997).
6. R. Broda, B. Fornal, W. Krolas, T. Pawlat, D. Bazzacco, S. Lunardi, C. Rossi-Alvarez, R. Menegazzo, G. de Angelis, P. Bednarczyk, J. Rico, D. De Acuna, P.J. Daly, R.H. Mayer, M. Sferrazza, H. Grawe, K.H. Maier, R. Schubart, Phys. Rev. Lett. **74**, 868 (1995).
7. H. Takai, C.N. Knott, D.F. Winchell, J.X. Saladin, M.S. Kaplan, L. de Faro, R. Aryaeinejad, R.A. Blue, R.M. Ronningen, D.J. Morrissey, I.Y. Lee, O. Dietzsch, Phys. Rev. C **38**, 1247 (1988).
8. S.J. Asztalos, I.Y. Lee, K. Vetter, B. Cederwall, R.M. Clark, M.A. Deleplanque, R.M. Diamond, P. Fallon, K. Jing, L. Phair, A.O. Macchiavelli, J.O. Rasmussen, F.S. Stephens, G.J. Wozniak, J.A. Becker, L.A. Bernstein, D.P. McNabb, P.F. Hua, D.G. Sarantites, J.X. Saladin, C.-H. Yu, J.A. Cizewski, R. Donangelo, Phys. Rev. C **60**, 044307 (1999).
9. J. Simpson, Z. Phys. A **358** (1997) 139.
10. D.C. Radford, Nucl. Instrum. Methods Phys. Res. A **361**, 297 (1995).
11. D.R. Haenni, H. Dejbakhsh, R.P. Schmitt, G. Mouchaty, Bull. Am. Phys. Soc. **29**, No.7, 1043, CC14 (1984).
12. H. Beuscher, W.F. Davidson, R.M. Lieder, A. Neskakis, C. Mayer-Boricke, Nucl. Phys. A **249**, 379 (1975).
13. W. Andrejtscheff, P. Manfrass, K.D. Schilling, W. Seidel, Nucl. Phys. A **225**, 300 (1974).
14. E.K. McIntyre, T.J. Hallman, K.S. Kang, C.W. Kim, Y.K. Lee, L. Madansky, G.R. Mason, Phys. Lett. B **137**, 339 (1984).
15. T. Ramsoy, J. Rekstad, M. Guttormsen, A. Henriquez, F. Ingebretsen, T. Rodland, T.F. Thorsteinsen, G. Lovhoiden, Nucl. Phys. A **438**, 301 (1985).
16. H.J. Riezebos, M.J.A. de Voigt, C.A. Fields, X.W. Cheng, R.J. Peterson, G.B. Hagemann, A. Stolk, Nucl. Phys. A **465**, 1 (1987).
17. T. Härtlein et al., Nuovo Cimento A **111**, 645 (1998).
18. B. Bochev, T. Kutsarova, R.M. Lieder, T. Morek, J.P. Didelez, Nucl. Phys. A **458**, 429 (1986).

19. A. Atac, J. Rekstad, M. Guttormsen, S. Messelt, T. Ramsoy, T.F. Thorsteinsen, G. Lovhoiden, T. Rodland, Nucl. Phys. A **472**, 269 (1987).
20. T. Ramsoy, A. Atac, T. Engeland, M. Guttormsen, J. Rekstad, G. Lovhoiden, T.F. Thorsteinsen, J.S. Vaagen, Nucl. Phys. A **470**, 79 (1987).
21. R. Bengtsson, S. Frauendorf, Nucl. Phys. A **327**, 139 (1979).
22. S.G. Nilsson, C.F. Tsang, A. Sobiczewski, Z. Szymanski, S. Wycech, C. Gustafson, I.-L. Lamm, P. Moller, B. Nilsson, Nucl. Phys. A **131**, 1 (1969).
23. A. Bohr, B.R. Mottelson, *Nuclear Structure*, Vol. **1** (Benjamin, New York 1969).
24. V. Velázquez, J.G. Hirsch, Y. Sun, M.W. Guidry, Nucl. Phys. A **653**, 355 (1999).